Available online at www.sciencedirect.com
ScienceDirect
Journal of Nuclear Materials 363–365 (2007) 1277–1282
journal of nuclear materials
www.elsevier.com/locate/jnucmat

Surface effects on graphite samples exposed to beryllium-seeded plasmas under transient power load on PISCES-B

R. Pugno [a,*], M.J. Baldwin [b], R.P. Doerner [b], J. Hanna [b], D. Nishijima [b], G. Antar [b]

[a] *Max-Planck-Institut für Plasmaphysik, IPP-EURATOM Association, Boltzmann str. 2, D-85748 Garching, Germany*
[b] *University of California at San Diego, La Jolla, CA 92093, USA*

Abstract

A transitory positive voltage biasing (called hereafter 'pulsing') is applied to a graphite target during deuterium plasma exposure in the PISCES-B linear device to simulate the heat pulse associated with ELMs. The effect of the pulsing on the suppression of chemical erosion and on deuterium retention is investigated, both in pure deuterium and in beryllium-seeded plasmas. In the presence of power transients, spectroscopic observation of CD molecular band at 430 nm and mass loss measurements indicate a shorter time for beryllium-induced suppression of chemical erosion. No effect on erosion due to pulsing is observed for pure graphite surfaces. Deuterium retention is found to be higher when pulsing is applied, by 60% during beryllium seeding and by 30% for pure deuterium. Infrared radiation emitted from the target surface indicates a modification of the surface morphology during the plasma exposure of the graphite samples and a smaller heated emitting area during the pulsing compared to the total exposed area.

PACS: 52.40.Hf

Keywords: PISCES-B; Beryllium; Carbon; Mixed-material; Chemical erosion

1. Introduction

The present ITER design employs beryllium as the main chamber wall material, and a combination of tungsten and carbon in the divertor. The beryllium is expected to be eroded from the first wall. It will then enter the SOL and be transported to the divertor, where it will interact with the divertor materials. In recent years a big effort was dedicated to the investigation of plasma interaction with ITER first wall materials [1,2] and of the effects of beryllium deposition/erosion/redeposition on plasma facing divertor materials and the concomitant formation of mixed-material surfaces. On the PISCES-B linear device, targets of different materials (W, C, Be) were exposed to beryllium-seeded deuterium plasmas and the dependence on

* Corresponding author.
E-mail address: Roberto.Pugno@ipp.mpg.de (R. Pugno).

0022-3115/$ - see front matter © 2007 Published by Elsevier B.V.
doi:10.1016/j.jnucmat.2007.01.243

beryllium concentration and on plasma parameters were investigated [2,3].

As one of the main findings, the exposing of graphite targets to plasmas containing small beryllium concentration (<0.1%) revealed the formation of a protective Be_2C surface layer which suppresses hydrocarbon formation and strongly reduces chemical erosion [4].

Though these multi-material layers may have a significant impact on ITER operation, little is known about the effects of ELMs on the alloy formation (in the case of W–Be interaction) and on the formation/stability of the Be_2C coating layer on carbon surfaces.

With this purpose, the EU–US collaboration on PISCES-B has been extended, and the effects of power transients on carbon targets have been investigated. Although the peak temperatures during the pulsing are lower than the ones foreseen for ITER ELMs, interesting qualitative trends are found.

2. Experimental setup

Grade ATJ isomoulded graphite target disks, 22 mm diameter and 2.8 mm thick, were exposed to the deuterium plasma flux in the PISCES-B device [2–4]. To simulate the ITER main chamber beryllium source, an evaporative neutral atomic beam source is used [3]. The amount of beryllium in the plasma is controlled by changing the temperature of the evaporative cell. A radially integrated axially resolved spectroscopy view enables the measurement of the axial distribution of D_γ (434 nm), Be I (457.3 nm), Be II (467.3 nm) lines and CD band (430 nm) intensity during the discharge.

The D_γ line intensity is used to verify the stationarity and axial density profile of the plasma. The CD molecule band intensity near the target is a measurement of the carbon chemical erosion. The plasma parameters n_e and T_e are obtained using a reciprocating Langmuir probe. The beryllium ion density is obtained from the Be II absolute intensity, using the photon efficiency coefficient from the ADAS database [5] for the measured plasma parameters.

Samples in PISCES-B are typically biased negatively during the plasma exposure to accelerate incident ions to a given energy. In parallel to the power supply for the negative biasing, a new pulsed power supply was installed to provide transient positive biasing to the target sample, drawing an electron current from the plasma [6]. A fast switch permits the reversal of the standard negative potential to the positive potential and back with a response time of about 1 μs. In the present configuration the shortest positive biasing pulse duration is 100 ms and the peak positive biasing voltage 50 V. The electron current drawn in the plasma is mainly controlled by the discharge electron density and for given plasma condition is nearly constant once it reaches the saturation value. The power during the pulsing is then proportional to the positive applied voltage.

The target temperature on PISCES-B is routinely measured by a thermocouple in contact with the back of the sample. The time response of the thermocouple is a few seconds, adequate for steady plasma exposure but not for measuring fast transients. Hence a new infrared spectrometer, consisting of a photodiode array detector working in the wavelength range 0.9–1.6 μm and a prism as dispersing element, was installed [6]. The light emitted from a circular spot on target surface, 6 mm diameter, is collected and focused into an IR optical fiber with 910 μm core diameter.

After each exposure the samples have been analysed *in situ* using a surface analysis system [7], which comprises an Auger electron spectrometer (AES), used primarily to investigate the surface composition, and an X-ray photo-electron spectrometer (XPS) that further allows the study of the chemical binding status of the surface materials. The samples were subsequently removed, weighted on a micro balance, and taken to a JEOL-JSM 6830 scanning electron microscope (SEM) to analyse changes in surface morphology. To quantify the effect of pulsing on the deuterium inventory, a thermal desorption mass spectrometer (TDS) was used. The samples were heated with a linear ramp of 0.29 K s^{-1} to a top temperature of 1050 °C, and the desorbed gas was gauged in a quadrupole residual gas analyser (RGA).

3. Measurement

A set of four graphite samples was exposed to similar plasma conditions (see Table 1), two with pure deuterium plasma (samples THC5 and THC6) and two with 0.13% beryllium concentration (THC7, THC8). For each of the two conditions one sample was exposed to the transient power loads (0.1 Hz frequency and 100 ms pulse length). The plasma parameters during the exposures were $T_e = 7$–8 eV, $n_e = 3.2$–4.0×10^{18} m^{-3}, ion flux= 3.5–4.0×10^{22} m^{-2} s^{-1}, $T_{average} = 500$–600 °C. The

Table 1
Summary of the exposure conditions (Be concentration and pulsing status), mass loss, experimental and predicted chemical erosion decay time and deuterium retention, for the analysed samples

Sample	Be concentration (%)	Pulsing	Mass loss (mg)	Exposure decay (s)	Scaling decay (s)	D retention (10^{20} at/m^2)
THC-5	0	Yes	20.1	n.a.	n.a.	12
THC-6	0	No	18.3	n.a.	n.a.	7.8
THC-7	0.13	No	5.2	83	76	4.9
THC-8	0.13	Yes	<1	17	76	11.6
THC-10	0.02	Yes	4.5	831	5470	n.a.

total plasma exposure time was 2500 s, corresponding to a deuterium ion fluence of 1×10^{26} m^{-2}. The target was biased to -50 V, corresponding to 40 eV impact ion energy [8], except during the pulsing when the averaged applied voltage was $+33$ V (± 10 V due to plasma impedance fluctuations) and the current about 20 A.

Assuming that most of the power during the pulsing is dissipated on the exposed target surface of 3.8×10^{-4} m^2, the electron power load density results in about 2 MW/m^2.

The startup phase of each discharge lasts a few minutes before reaching stable plasma and target conditions. Also after the beryllium evaporative cell is opened, a few tens of seconds are necessary to reach steady state.

4. Analysis

In Fig. 1 the temporal evolution of the CD intensity shows the progressive reduction of chemical erosion after the beryllium oven opening [9]. The characteristic time of protective beryllium layer formation for the THC8 sample (with pulsing) is clearly shorter than THC7 (same condition but no pulsing). Unfortunately, the decay for the THC8 sample is 17 s, comparable to the re-equilibration time of the beryllium evaporative cell. An additional exposure at lower beryllium concentration (0.02%) was done, giving a layer formation time of 831 s. This is eight times shorter than the value of ~6900 s expected from the scaling in [10] for the surface average temperature of 510 °C. Assuming the scaling to be valid for $T_{surface} = 1100$ °C (maximum temperature during the pulsing), the predicted decay time would be ~500 s, fourteen times faster than during the inter-pulse conditions. Since the integrated time during the pulsing is 20 s to be compared with 2000 s inter-pulsing (one 100 ms pulse every 10 s), the contribution of the pulsing (assumed in steady state) to the total decay time would be about 15% of the inter-pulse DC exposure decay time. The reduced formation time of the Be_2C protection coating during the pulsing is more than a pure temperature effect, as predicted by the scaling.

In Fig. 2 the XPS carbon-1 s spectra of the four samples are shown. Both beryllium-exposed samples (THC7,THC8) show a complete carbidization of the

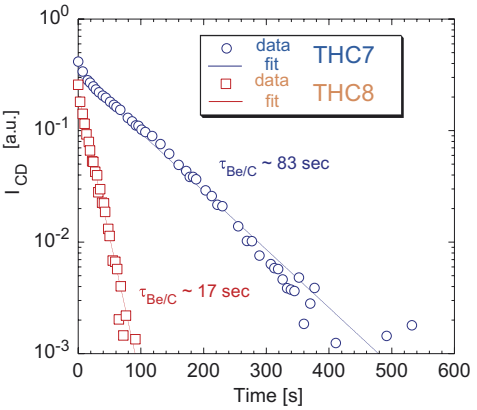

Fig. 1. The temporal decay of the CD band intensity (background subtracted and normalised to D_γ intensity) during beryllium-seeded plasma exposure ($c_{Be} = 0.13\%$) is shown for the samples THC7 (no pulsing) and THC8 (with pulsing).

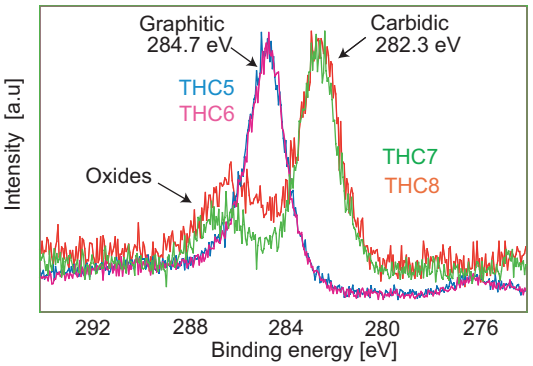

Fig. 2. C 1 s X-ray photo-electron spectra taken on graphite exposed to pure deuterium plasma (THC5, THC6) and beryllium-seeded plasma (THC7, THC8, $c_{Be} = 0.13\%$). The pulsing exposed samples (THC5, THC8) do not differ from the corresponding samples without pulsing (THC6 and THC7 respectively).

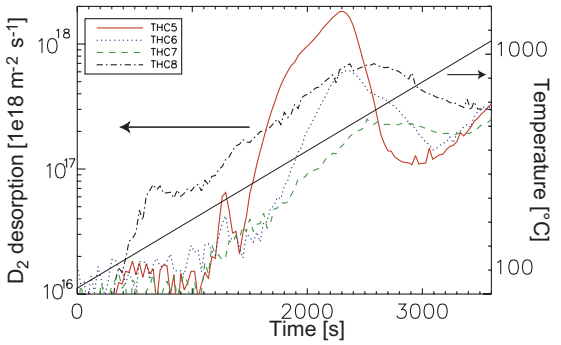

Fig. 3. Thermal-desorption-spectrometry profiles for graphite target exposed to pure deuterium plasma (THC5, THC6) and to beryllium-seeded plasma (THC7, THC8, $c_{Be} = 0.13\%$), with pulsing (THC5, THC8) and without (THC6, THC7).

graphite surface (i.e. Be_2C composition), in agreement with previous Be-seeded exposure results [7], while the THC5 and THC6 samples without beryllium injection are in graphitic status. The pulsing shows no effect concerning the XPS spectra. The AES measurements give Be/C ratios of 1.7 and 2.1 for, respectively, the DC and the pulsed case. Both values are close to the expected stoichiometric value for a Be_2C surface. The mass loss measurement (see Table 1) shows a strong reduction of erosion in the case of pulsing with beryllium, confirming faster formation of the protective Be_2C layer.

For the pulsed samples the TDS measurements (Fig. 3) exhibit a higher deuterium retention. The inventory increase is 60% for the beryllium-seeded case and 30% for pure deuterium.

The SEM analysis of the exposed targets shows a modification of the surface morphology during the plasma exposure of the ATJ graphite. The flake-like surface of the pre-exposure sample (Fig. 4(a)) changes to a cone-like structure (Fig. 4(b)) after deuterium plasma exposure [7]. In presence of beryllium the cone-like structure is replaced by a more uniform surface (Fig. 4(c)). As will be discussed in the next paragraph, the modification of the surface morphology has an impact on the measured surface temperature.

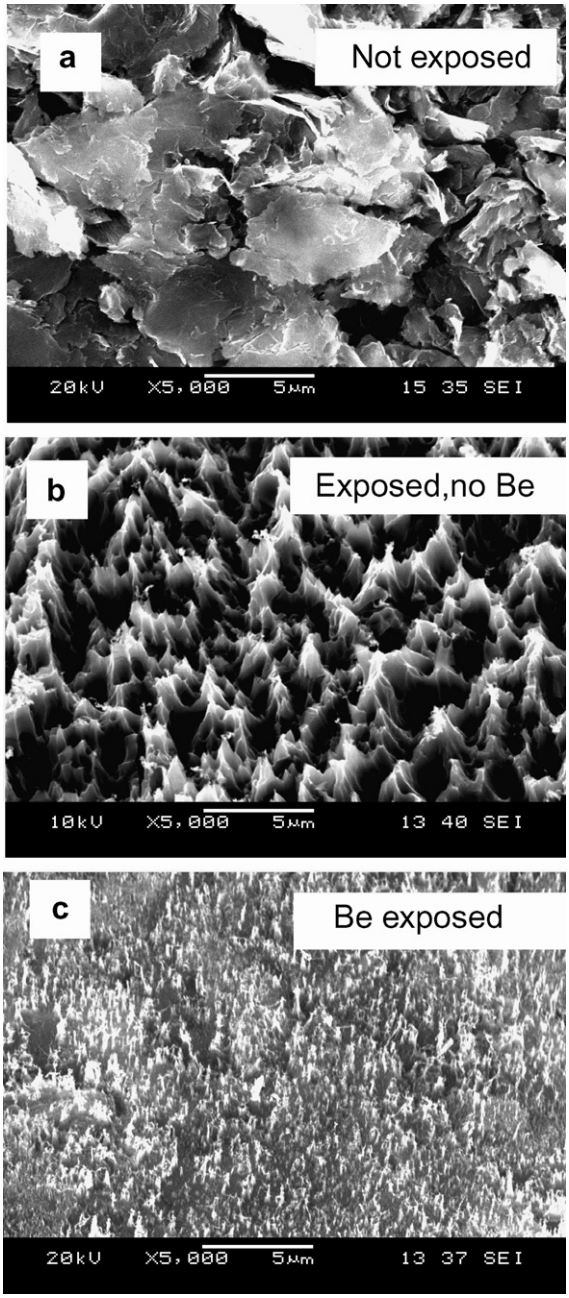

Fig. 4. Electron micrograph of (a) unexposed graphite target, (b) deuterium plasma exposed graphite target and (c) beryllium-seeded deuterium plasma exposed graphite target.

5. IR analysis

The measured infrared radiation intensity can be described using the formula:

$$I(\lambda, T) = \alpha \cdot \frac{c_1}{\lambda^5 \cdot [e^{c_2/\lambda \cdot T} - 1]},$$

with $\alpha = K \cdot \Omega \cdot A \cdot \varepsilon$, where K the system efficiency, Ω the observation solid angle, A the observed area, ε the material emissivity, λ the wavelength, T the surface temperature, and c_1 and c_2 are the first and second radiation constants. The IR spectrometer was wavelength calibrated using a mercury gas lamp. The intensity calibration was achieved by plasma heating the graphite sample at different temperature in semistationary condition (sample

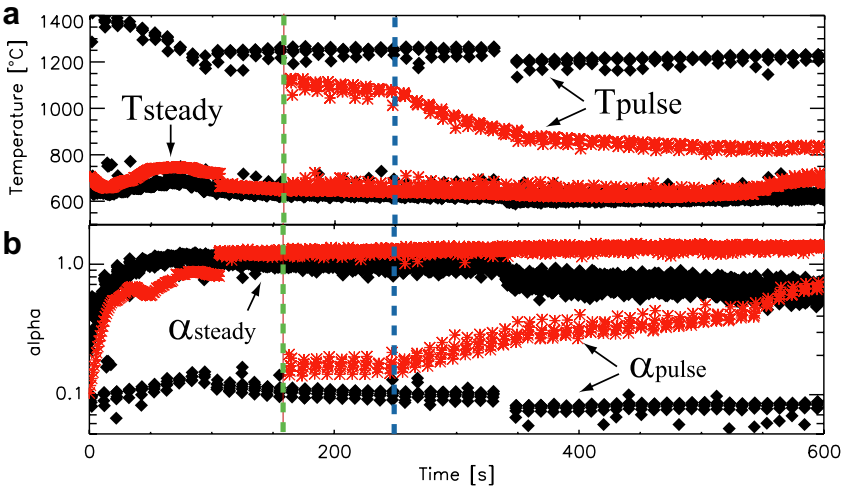

Fig. 5. The time evolution of the fitted parameter T (a) and α (b) during the plasma exposure are shown for the sample THC5 (black) and THC8 (red). The excursion are caused by the pulsing. The pulsing values are the higher temperatures and the lower αs. The lower temperatures and the higher αs are during the DC exposure between pulses. The beginning of pulsing (green) and of beryllium exposure (blue) for THC8 are shown. THC5 (black) was exposed to pure deuterium plasma and pulsed from the beginning.

holder active cooling off) and using the thermocouple temperature as reference.

In Fig. 5 are shown the time evolution of the two fit parameter T and α for the samples THC5 and THC8. The pulsing starting time (green)[1] and beryllium exposure (blue) for the sample THC8 are also shown. For each sample the highest temperatures are during pulsing (T_{pulse}), while the lowest temperatures reflect the steady state temperature (T_{steady}). For the THC5 sample (pure deuterium plasma), both T_{pulse} and T_{steady} increase slightly during the discharge. For the beryllium exposed sample (THC8) T_{steady} is constant and not affected by the beryllium injection, while T_{pulse} shows an evident reduction following the beryllium exposure.

Interestingly, the fitting coefficient α, which is about 1 at the beginning of the exposure with no pulses, as expected from the calibration procedure, becomes much smaller during the pulsing (Fig. 5(b)). For the pure graphite surface α_{steady} decreases from 1.1 to 0.3 (after 2500 s), while during the pulsing $\alpha_{\text{pulse}} \simeq 0.1$. The ATJ graphite emissivity is 0.8–0.9 and has a weak dependence on temperature [11]. A variation of more than a factor of 2 in the α coefficient can hardly be explained by a change in the graphite surface emissivity. The system efficiency and the geometry are unchanged and the only possible explanation is a change in the heated surface. The change of α_{steady} during the sample exposure is likely to coincide with the modification of the surface morphology due to the chemical erosion and the buildup of the peak-like structure (Fig. 4(b)).

A non-uniform heating of the surface would give a higher measured temperature with respect to the average surface temperature due to the strong non-linear behaviour of blackbody radiation [12] and an apparent lower emissivity. The *ab initio* difference of α_{steady} and α_{pulse} indicate a preferential heating of a part of the surface during the pulse throughout the exposures. The peak-like structure could modify the electric field distribution at the surface and cause a preferential heating of the peaks, possibly with different characteristics for electron heating (positive biasing) and ion heating (negative biasing).

In the presence of beryllium the peak-like morphology does not appear (Fig. 4(c)), and no evident change in α_{steady} is observed. The increase of α_{pulse} during the beryllium exposure, concurrently with a decrease in T_{pulse}, is consistent with a more uniform distribution of the power on the surface and a lower peak temperature.

6. Conclusion and outlook

Power transients with sample peak temperature between 800 and 1400 °C have been applied during deuterium plasma exposure of graphite targets, with and without beryllium impurity seeding.

[1] For interpretation of color in Figs. 1–3 and 5, the reader is referred to the web version of this article.

As observed from mass loss and optical spectroscopy, the power transients reduce the formation time of the Be_2C layer and hence strongly reduce the chemical erosion. No indication of removal of the protective layers is found at the present temperature range. Approaching the Be_2C decomposing temperature (2100 °C), different behaviour could arise.

The change in the surface morphology is found to affect the infrared spectra. The chemical erosion induced peak-like surface structure shows a preferential heating of a reduced area during the pulsing. In the presence of beryllium seeding, the target surface becomes more uniform and the peak temperature during the pulsing is reduced.

An increase in deuterium retention is found during the application of the power transients. Again, due to the presence of competing effects which could increase or decrease the deuterium trapping, such as thermal desorption and bulk diffusion, no extrapolation to ITER can be done yet.

A new power supply will be installed, which will allow to increase the positive biasing to 330 V. This should increase by a factor of 10 the power load on the target. Temperature effects closer to ITER conditions will thus be investigated.

Acknowledgements

The authors wish to acknowledge and thank for the support and dedication shown by the technical staff of PISCES-B. This work is supported by the US-DOE under the contract DOE DE-FG03-95ER-54301 and the TASK TW5-TPP-CARWBER of the EFDA technology programme.

References

[1] A. Loarte et al., J. Nucl. Mater. 337–339 (2005) 816.
[2] R.P. Doerner et al., J. Nucl. Mater. 337–339 (2005) 877.
[3] R.P. Doerner et al., J. Nucl. Mater. 342 (2005) 63.
[4] K. Schmid et al., J. Nucl. Mater. 337–339 (2005) 862.
[5] H.P. Summers et al., Atomic Data and Analysis Structure – User Manual, Rep. JET-IR(94), JET Joint Undertaking, Abindon, 1994.
[6] J. Hanna et al., Rev. Sci. Instrum. 77 (2006) 123503.
[7] M.J. Baldwin et al., J. Nucl. Mater. 358 (2006) 96.
[8] K. Schmid, J. Appl. Phys. 92 (2005) 064912.
[9] M. Baldwin, NF 46 (2006) 444.
[10] D. Nishijima et al., J. Nucl. Mater., these Proceedings, doi:10.1016/j.jnucmat.2007.01.177.
[11] Y.S. Touloukian, D.P. DeWitt, Thermal Radiative Properties: Nonmetallic Solids, vol. 8, IFI Plenum, New York, NY, 1970.
[12] Reichle et al., J. Nucl. Mater. 313 (2003) 711.